Thermal Grease Evaluation for ATLAS Upgrade Micro-Strip Detector

G. Barbier, F. Cadoux, A. Clark, D. Ferrère, S. Pernecker, E. Perrin, K.-P. Streit, M. Weber

DPNC, University of Geneva

ATL-UPGRADE-PUB-2010-002
04 February 2010

1. INTRODUCTION

The current ATLAS SCT strip silicon detector[1,2] has been designed to operate for 10 years at the LHC with a luminosity of up to 3 x 10^{34} cm^{-2} s^{-1} and to withstand a 1 MeV equivalent neutron fluence of 2 x 10^{14} n_{eq} /cm^2. In a second phase (sLHC), a 10-fold increase in the peak luminosity is expected, and for this reason the ATLAS detector will be upgraded. This upgrade is foreseen for 2018 and R&D has started for the new Inner Tracking Detector (ID) of ATLAS. For the ATLAS ID upgrade[3] the complete tracker will be rebuilt using silicon detectors: strips and pixels. An important R&D challenge is to ensure that all components of the silicon modules and associated electrical, thermal and mechanical infrastructure withstand the expected radiation level. A specification has been defined for operability up to a fluence of 10^{16} n_{eq}/cm^2 for the pixel and 10^{15} n_{eq}/cm^2 for the silicon micro-strip detector (this takes account of a 50% uncertainty in the expected fluence).

The ID will operate at a temperature of ~ -10°C, and in many ID designs (as well as the existing SCT) grease interfaces are used to minimise distortions during thermal cycling while ensuring good thermal contact between the silicon modules and the cooling pipes. A power of 0.3W/chip is currently used in the FEA simulations but half of this value is targeted for the next design of the ABCN in 130nm technology. Therefore the expected power per module should not exceed 24 Watts.

An important goal of the R&D module program[4] is to select a thermal grease having mechanical and thermal properties that guarantee a good module contact during 10 years of operation in this severe radiation environment. Two parameters have to be evaluated: the mechanical properties (mainly the viscosity) and the thermal conductivity.

A program of test measurements has been established to compare several heat sink compounds and to check their suitability for the detector upgrade.

This report will focus on the thermal properties of three heat sink compounds.

2. THE EXPERIMENTAL SET-UP

2.1 Description of the experimental set-up

An essential measurement for any candidate heat sink compound (grease) is to measure the deterioration of thermal conductivity following irradiation.

The experimental set-up used for this measurement consisted of two identical channels, A and B (see Figure 1). This allowed a direct measurement of the difference of the thermal conductivity of the samples in the channels A and B. The apparatus could be used in two operational modes:

1) The measurement of the conductivity of the irradiated grease relative to the identical sample of non-irradiated grease

2) The measurement of different samples against a “standard”, this also enabled the monitoring of the stability of the whole set-up over time.

We have chosen the latter mode with the non-irradiated Dow-Corning heat sink compound DC340[5] as "standard" in channel B and all other samples in channel A. This compound was

chosen as a standard comparison because of its use as thermal grease for the existing SCT detector.

As the set-up was built to measure the difference of thermal conductivity between two samples, it was also possible to determine the absolute values for the thermal conductivity by the use of reference samples with well-established thermal conductivity values.

Each channel consisted of a "heating" and a "cooling" block, both made of aluminium. They were separated by a Plexiglas spacer, which defined the volume for the samples to be measured.

A polyimide thermo-foil[6)] glued on the outer face of the heating block was used as a tuneable heat source. The heat flux through the samples was absorbed in the cooling water flowing through the cooling block. The two channels were thermally decoupled by a silicone hosepipe.

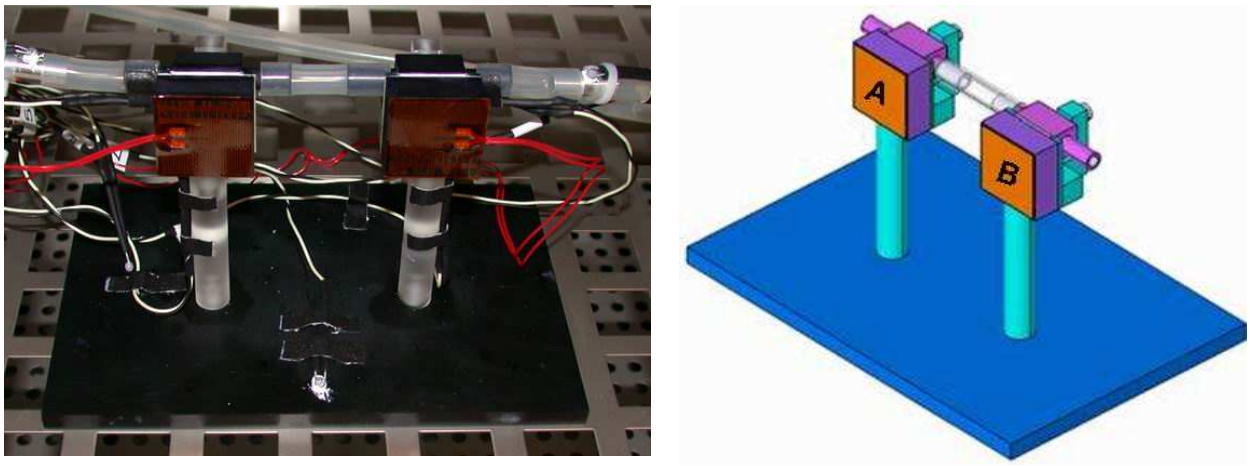

Figure 1: Set-up for the grease measurement. In this case, both channels were loaded with the white DC340 grease. As illustrated on the right hand side, A channel is on the left and B channel is on the right when the polyimide thermo-foils are in front.

The temperature distribution across each of the samples was measured by “Negative Temperature Coefficient” (NTC) thermistors that were glued on the heater and on the cooling blocks. Additional NTC thermistors monitored the water temperature at the entrance and exit of the cooling block, as well as the air temperature around the blocks.

The whole apparatus was enclosed in a Styrofoam box that was placed in a climate chamber. The Styrofoam box confined the air volume around the set-up and shielded the apparatus against the forced convection in the climate chamber.

The aim of these measurements was to establish differences in the thermal conductivity with an accuracy of the order of 5%. Detailed thermal FEA simulation studies with Abaqus[7)] and CATIA[8)] software were made to optimize the experimental set-up and to compare the measurement results. These simulations also identified the temperature range where the desired sensitivity could be achieved. In addition the simulation calculations enabled an estimate of additional heat exchange effects, such as radiation and convection, which significantly affect the measurements but cannot be measured directly.

A thermal camera has been used as a complementary tool to map the thermal distribution of the set-up and to control its homogeneity. In order to have a good response to the thermal camera the surfaces of the aluminium blocks were anodised with a black layer. During the measurements in the sealed Styrofoam box the thermal camera was not usable.

2.2 Calibration of the sensors

A total of 8 NTC thermistors were used for this set-up. They were calibrated against the climate chamber in 5 ^{o}C steps as shown in Figure 2. Using a linear interpolation between the measured points resulted in a maximum spread of 0.1^{o}C between the different NTC thermistors. This uncertainty is given by the limitation of the read-out electronics (0.05 ^{o}C /bit) and the precision of the climate chamber temperature display (0.1 ^{o}C)

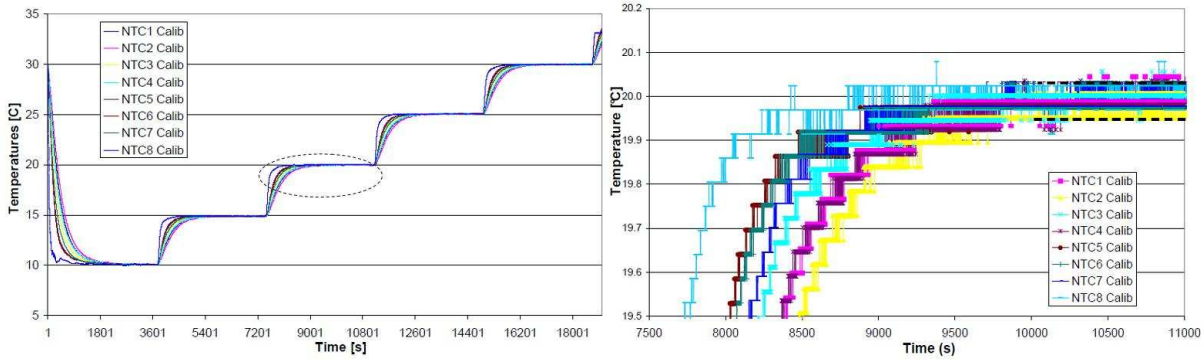

Figure 2: Calibration of the thermo-sensors against the climate chamber. The right hand-side shows a magnification of the dashed area on the left hand side.

In future measurements the precision of the read-out ADCs will be increased by a factor of four. This will decrease the measurement errors to the level of the actual systematic uncertainties (see chapter 6.3)

3. THE INFLUENCE OF PERTURBATIVE HEAT EXCHANGES

3.1 Radiation and convection

Radiation and convection occurs whenever the surface of a body is exposed to surrounding material of different temperature. These contributions can become significant if the set-up is not properly adapted.

The heat transfer by radiation is proportional to the exposed surface, the emissivity of the surface and the fourth power of the absolute temperature. The emissivity of a body which has a dark aspect can be close to unity.

Heat exchange via convection is proportional to the exposed surface, the temperature difference and a heat exchange coefficient which is itself dependent of the temperature and the exact geometry. For natural convection of air the heat exchange coefficient is approximately 5W/m^{2}K.

3.2 Measurement and FEA thermal modelling of radiation and convection

Radiation effects were initially observed using a prototype of the set-up where a heating resistance was used as the power source (see Figure 3). In this case, a sample of Dow Corning DC340[5)] heat sink compound was used in channel A and B. One clearly sees the deviation from a linear behaviour due to the power loss via radiation of the heating resistance. For example, the temperature of the resistance was measured with the thermal camera to be ~ 40 ^{o}C at a power of 1 W, whereas the resistive film remained at ~ 23 ^{o}C (see Section 4.2).

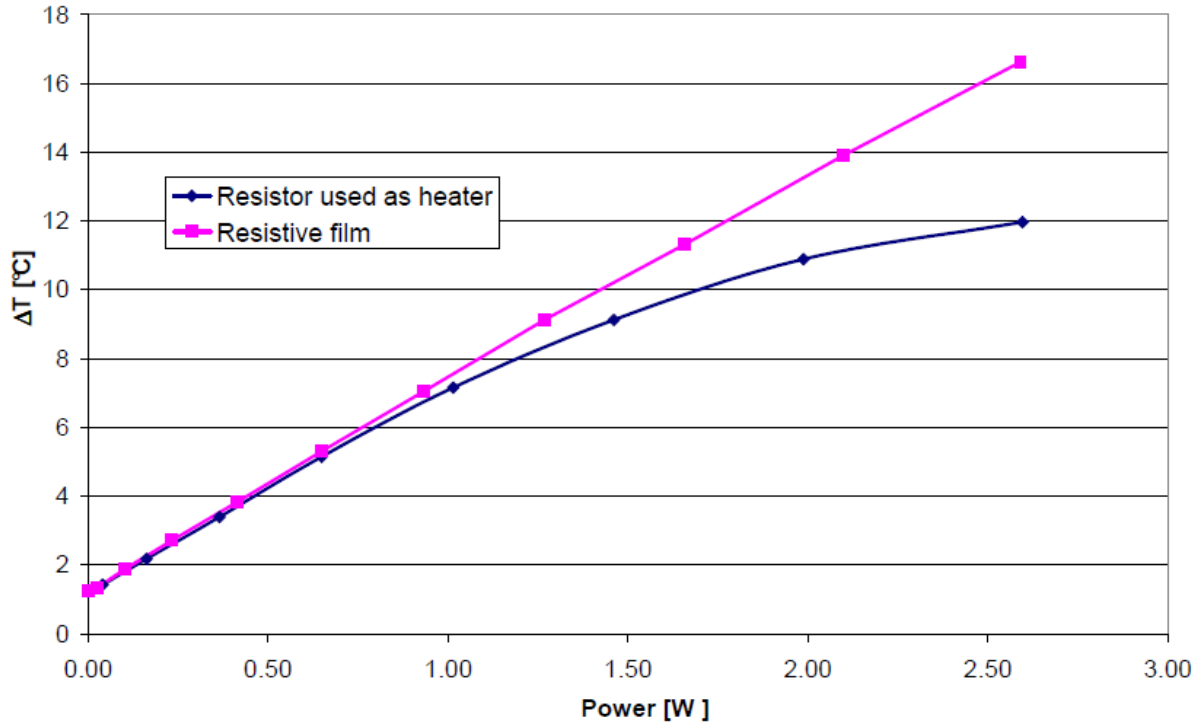

Figure 3: Temperature gradient between the heating and cooling block for the resistive film and the thermal resistance as heating source for DC340 compound (outside climate chamber)

The effect of convection was observed in the early stage of the experiment, when the set-up was placed inside a 20mm Styrofoam box without the use of the climate chamber. The temperature gradient through the samples as a function of the heater power could be fitted by a straight line, indicating a residual heat flux between the heating and cooling blocks at zero power (see Figure 4). This effect was mainly produced by convection between the surrounding air at room temperature and the heating block with a typical temperature difference of 5 to 6°C.

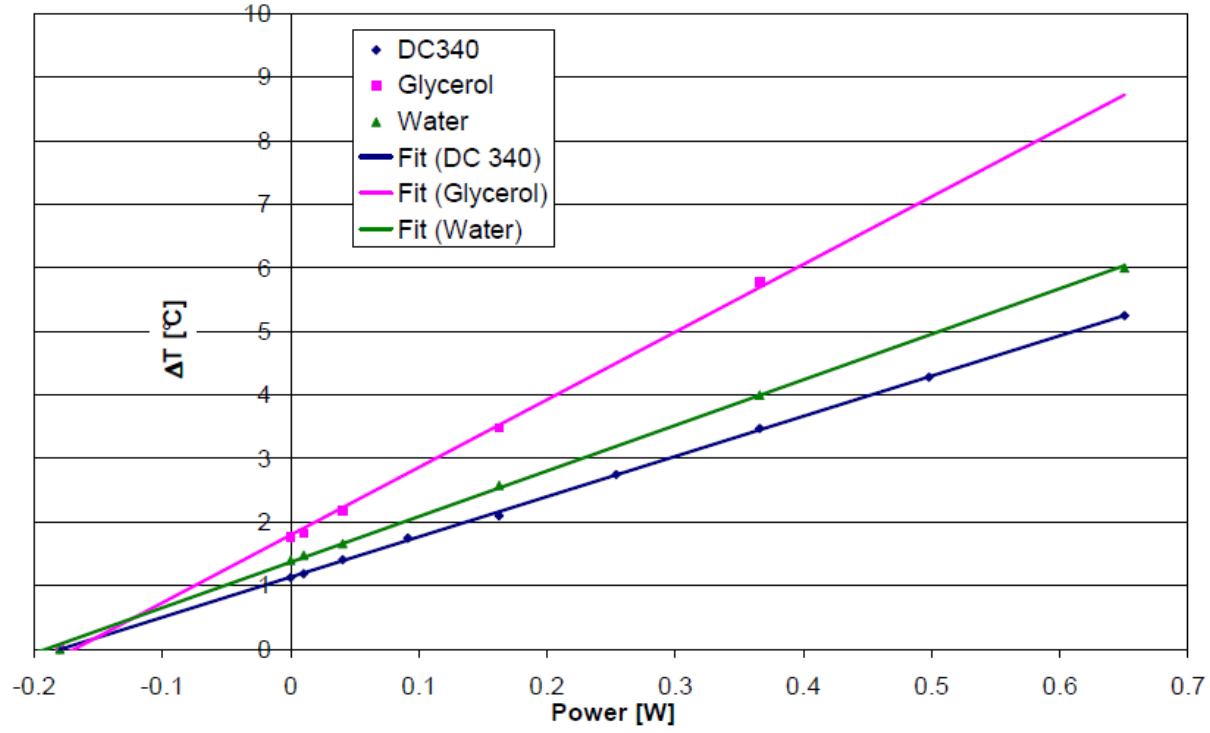

Figure 4: Temperature gradient between the heating and cooling block when the Styrofoam-box was outside the climate chamber.

To study these phenomena the water coolant temperature was varied in steps of 3°C from 10 to 25°C without any power on the heater blocks. The temperature gradient through the grease layers as function of the air temperature is shown in Figure 5. The expected gradient was evaluated using the Abaqus FEA simulation tool, assuming a heat transfer coefficient h = 5 W/m^{2}K and an emissivity ε = 0.8. The measurement and the FEA simulation agree well in shape within the experimental error of 0.1 ^{o}C.

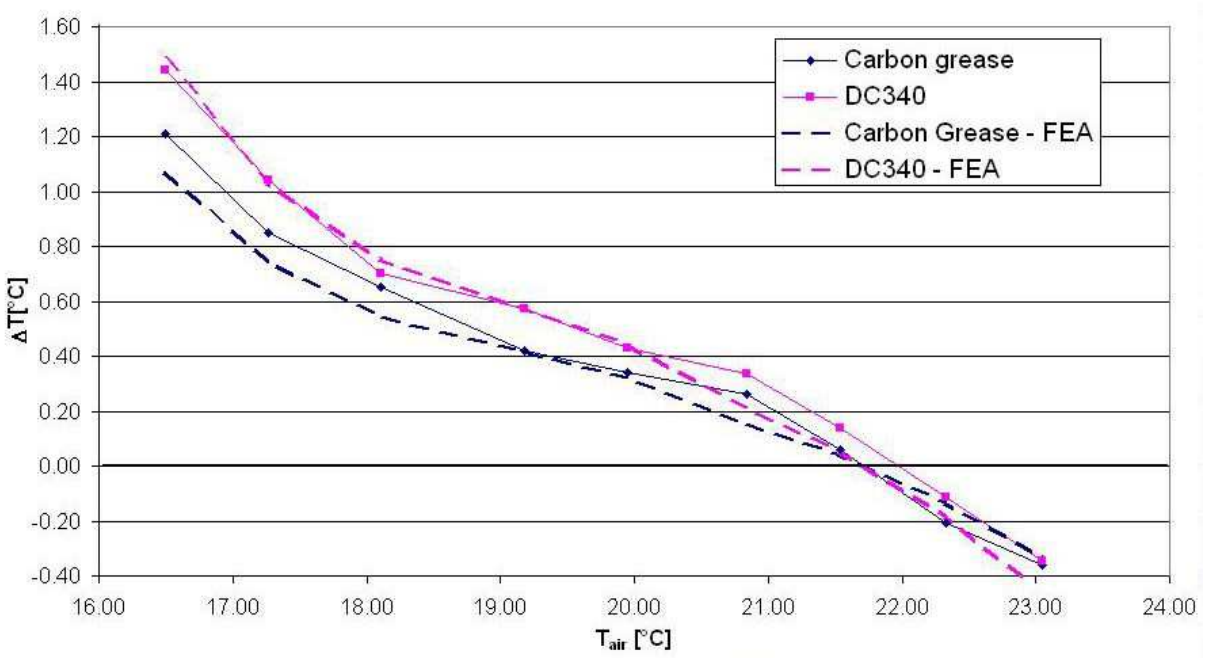

Figure 5: Temperature gradient through the grease layer as function of the air temperature in the Styrofoam box.

To minimize the effects of radiation and convection, a climate chamber was used to adjust the air temperature inside the Styrofoam box to the temperature of the heating-blocks.

4. THERMAL CONDUCTIVITY MEASUREMENTS OF VARIOUS COMPOUNDS

4.1 Experimental procedure

The channel B of the set-up, as shown in Figure 1, always contained a sample of DC340 to monitor the stability of the set-up with time.

For each material sample in channel A several data points were collected, varying the power P on the heating films. The power on the thermo-foil heaters was adjusted to produce the same temperature on the two heater-blocks. The air temperature inside the Styrofoam box was also tuned to the temperature on the heater-blocks by the use of the climate chamber. This allowed minimizing the power-loss due to convection and radiation in the apparatus. The temperature difference ΔT between heater-block and cooling-block was measured for both channels as a function of the heater power.

For each material sample the temperature differences ΔT were fitted as a function of the injected power with a straight line through the origin, including all data points for the sample. The result of these fits determined the effective thermal resistance ΔT/P of the samples. This effective thermal resistance was compared to results of FEA simulations for different values for the thermal conductivity.

4.2 Measurement of the thermal resistance and thermal conductivity of the DC340 heat sink compound.

Initial measurements were made using the Dow-Corning heat sink compound DC340[8)]. This compound was chosen as a standard comparison because of its use as a thermal grease for the existing SCT detector.

Figure 6 shows the data collected for the DC340 compound in channel B. From the raw data an effective thermal resistance $\Delta T/P = (8.24 \pm 0.17)\ ^{o}C/W$ was measured. The error is purely statistical and the straight line serves only to guide the eye.

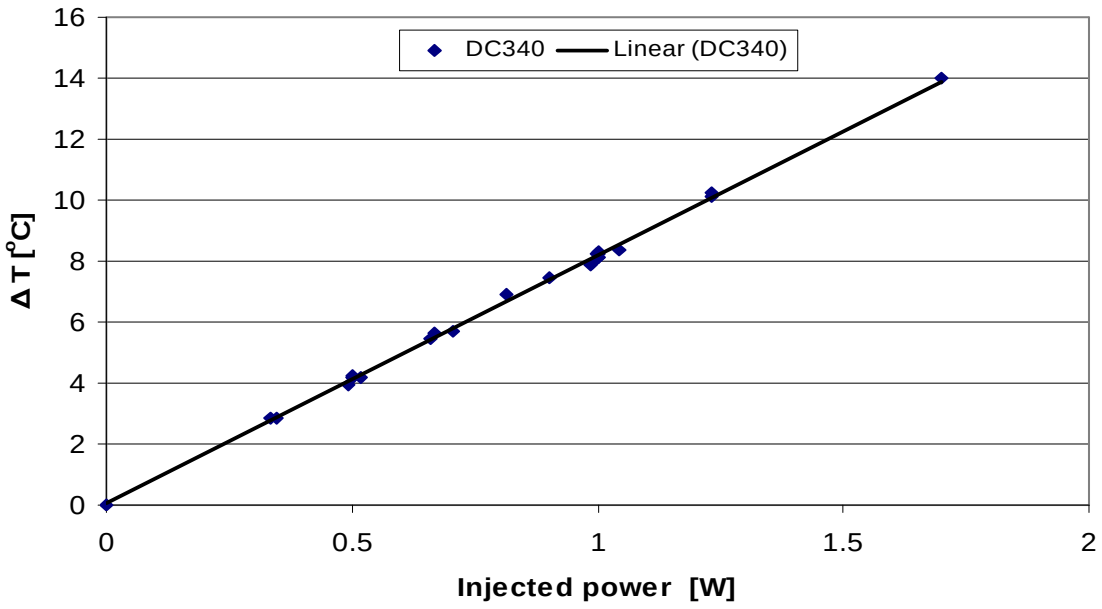

Figure 6: Effective thermal resistance of DC340 (all data points of channel B)

The measurement where both channels were loaded with DC340 revealed an asymmetry of the overall thermal resistances between channel A and B. To achieve the same temperature on both channels channel A consumed ~5.0 % less power than channel B. This difference was attributed to the adhesive quality of the scotch surface of the heater film. Figure 7 shows the temperature distribution on the two heater films with a power of 1 W on both channels as recorded by a thermal camera. One can clearly see the "hot" spot of ~37°C at the lower right corner in channel B indicating that the thermal resistance to the heater-block is increased.

The average temperature difference recorded by the camera between the heat film and the air (same temperature as the heating-block), is about 1.5–2°C. From the Abaqus simulation, a power loss of ~ (2.9 x ΔT) mW is expected due to convection on the back of the heater film and ~ (1.06 x ΔT) mW due to radiation. This means that there is a total power loss of ~8 mW on the back of the heater film. A correction of 1% was applied for channel A.

At the hot spot, an ~25 mW power loss is recorded, that is half of the difference in power (i.e. 2.5%) to achieve the same temperature on both heater blocks.

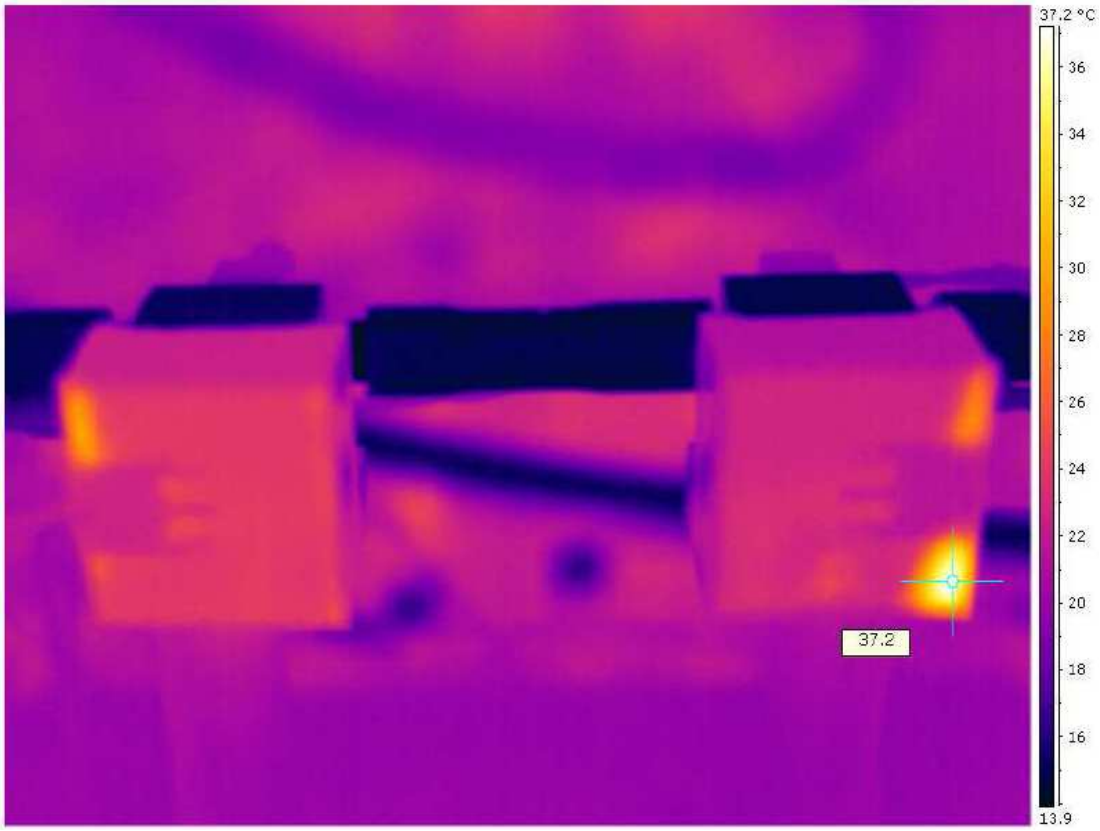

Figure 7 : Thermal distribution of the heater-blocks with DC340 filling at 1 W as seen by the thermal camera.

The polyimide FEP heater film[6)] specifications include:

- A resistance tolerance of ±10 %, including the internal FEP adhesive and a pressure sensitive adhesive for fixation. The two films used had a resistance difference of 2 %.
- A thickness specification of < 300 µm, including the 50 µm Polyimide layer, the 30 µm FEP layer and an adhesive foil backing of ~100 µm. A difference of 5 µm in the path to the heater block would produce a difference in the temperature drop of 3-4 %, that is between 0.06 and 0.08 ^{o}C at 1 W, at the limit of sensitivity.

These uncertainties will be included in the discussion of the systematic uncertainties (Section 4.6).

Figure 8 shows the thermal resistance of the DC340 sample in channel B during the measurements of the different material samples, after the correction of 3.5 % power loss discussed earlier, together with the measurement for DC340 in channel A.

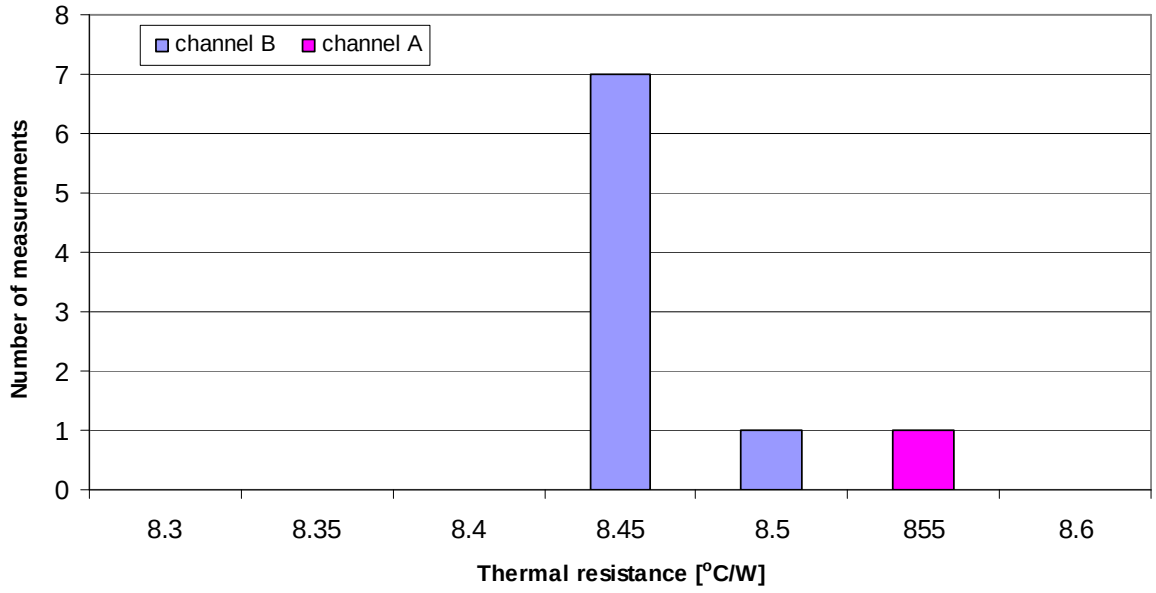

Figure 8: Thermal resistance of the DC340 compound (all measurements).

The thermal conductivity measured for the DC340 compound is shown in Figure 9.

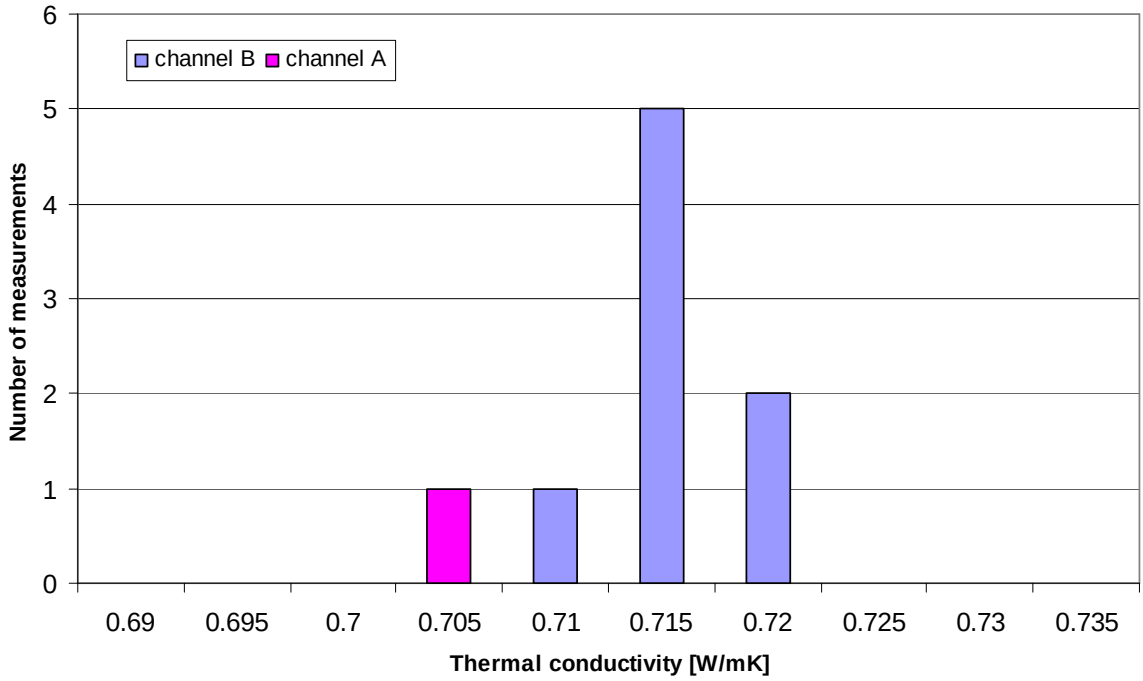

Figure 9: Measured thermal conductivity of the DC340 compound.

The values from channel A and B (0.706 and 0.719 W/mK respectively) agree well within the estimated error of 4.8 % (see below) and are averaged in the final result (see Table 3).

4.3 Description of heat sink samples measured

The reason for an early selection of grease compounds is based on the fact that this material is one of the key parts for the thermal and mechanical aspect to link the module to the cooling pipe. The validation tests can be long due to the irradiations to be performed and thermal and mechanical tests to be made.

Three heat sink compounds, as listed in Table 1, have been investigated so far, but only two have been irradiated. The Fischer graphite compound was very attractive because of its quoted thermal conductivity. The other 2 compounds have been used in the current ATLAS experiment for strip and pixel detectors[11]. The other fluids used in the set-up (Table 2) are for measurement crosschecks for example water, glycerol and silicon oil.

Material	***Datasheet thermal conductivity [W/mK]***	***Comments***
DC340[5]	0.4 to 0.6	Used in ATLAS SCT and other experiments. Silicon based compound, zinc oxide filled.
Fischer WLPG[9]	10.5	Not known to be used in High Energy Physics experiments. Organic oil, graphite filled.
CGL 7018[10]	>4	Used in ATLAS Pixel and other experiments. Non silicon based compound, aluminium nitride filled

Table 1: List heat sink compounds selected for this test.

4.4 Summary of measurements

The numerical values of the thermal conductivity measured for the different samples are summarized in Table 2, taking account of the corrections described and the known sources of systematic uncertainty.

Sample	**Comments**	**Table values [W/mK]**	**Reference**	**Measured thermal conductivity [W/mK]**
Silicon oil L-45 (Union Carbide) (19 ^{o}C)	viscosity unknown	0.163 (19 ^{o}C)	data sheet (7cstk)	0.159 ± 0.011
Glycerol (16 ^{o}C)		0.292	physics and chemistry handbook	0.286 ± 0.017
H2O (18 ^{o}C)	deionised water	0.597 (18 ^{o}C)	physics and chemistry handbook	0.587 ± 0.028
Dow Corning DC340 (16 ^{o}C)	pasty – white Silicone compound + zinc oxide filler	0.42 - 0.59	2 data sheets from Dow Corning	0.717 ± 0.034
DC 340 irradiated(16 ^{o}C)	polymerized different geometry			0.803 ± 0.0591
WLPG (Fischer) (16 ^{o}C)	pasty – black organic oil + graphite	10.5	data sheet	1.209 ± 0.058
WLPG irradiated (17 ^{o}C)				1.051 ± 0.050
AI Technology CGL 7018 (16 ^{o}C)	pasty – grey non silicone grease + AlN filler	>4.0	data sheet	1.178 ± 0.057

Table 2: Thermal conductivity of the tested samples. The measurements of Glycerol and water allowed verifying the absolute scale of the thermal conductivity.

A comparison has been made with samples of two well-known materials:

- H_2O: measured 0.587 ± 0.028 W/mK, nominal value 0.597 W/mK (18^oC)
- Glycerol: measured 0.286 ± 0. 017 W/mK, nominal value 0.292 W/mK

The measurements are in good agreement with the established values for both materials and demonstrate that the absolute calibration is correct.

The values given in Table 2 for the Union Carbide L-45 correspond to the oil with a viscosity of 7 cstk (mm^2/s). It should be noted that silicon oils are commercialized with different viscosities under the same name. The thermal conductivity of silicon oils with low and medium viscosities (i.e. < 5000 cstk) increases as a function of viscosity. Since the viscosity of the measured sample is not known, no conclusion can be made on the basis of the measured value.

Details on the irradiated samples are discussed in Section 5.

4.5 Comments on the Measurement Error

The limitation in ΔT represents an uncertainty of between 0.7% and 5% in the ΔT range between 2°C and 15^oC. The resistance of the thermo-foils was measured with a precision of 0.07 ‰ and the voltage supply was measured with a precision of (1-2) ‰. Therefore the error on the power measurement is less than 0.4 ‰. The various data points of each sample were fitted with a straight line to determine the thermal resistance which led to a maximum error on ΔR of 1.2 %.

4.6 Systematic uncertainties

Several systematic effects on the measurement accuracy were investigated:

a) *Geometrically uncertainties.*

The thickness of the samples (1.13 mm) was determined by the thickness of the Plexiglas-spacer (1mm) and a double-sided tape (0.13 mm) which fixed the spacer on the heating-block. The reproducibility of the thickness for different samples was estimated to be 10-20µm. This corresponds to a geometric uncertainty of (1-2) %.

The difference in power consumption of the two channels for the DC340 compound to produce the same temperature on the heater-blocks could reflect a difference of the thickness of the two glue-layers of the heater films of 0.005 mm. The difference of 2.5% which is not attributed to convection and radiation is considered as a possible systematic uncertainty.

For all samples, except the irradiated DC340 compound, the geometry of the sample was given by the probe volume of 17 x 10 x 1.13 mm^3. As the DC340 had polymerized after irradiation, we used a slice of approximately 1.96 mm thickness (± 5 %) and 10 mm diameter and clamped it between the 2 blocks. The material had remained elastic and a good thermal contact could be achieved under slight pressure. The sample had approximately twice the thickness and only half of the surface compared to the other material probes. It showed an effective conductivity of about 25% of DC340 in the set-up. A geometric uncertainty of 5 % is attributed to the measurement of the irradiated DC340 compound.

b) *Convection and radiation*

The air temperature inside the Styrofoam box was adjusted to the temperature of the heater blocks (the biggest parts in the heat path). Therefore energy exchange due to radiation and convection could only occur at surfaces which had a different temperature than the ambient air (the heater film, the cooling blocks and the hose-pipe). The monitoring of the in- and out-going

water temperature in the Styrofoam box showed a variation of 5% with temperature in the climate box (due to heat exchange with the hose-pipe inside the climate chamber). Inside the Styrofoam box the coolant temperature did not change between the entrance and exit thermistors. The temperature difference between the heater block and the heating film seen by the thermal camera allowed an estimate of the energy loss due to the combined effect of radiation and convection to be less than 3.5% for channel B and 1% for channel A (film coefficient 5 W/m^2K, emissivity 0.8). The relatively high value for the emissivity accounts for the black surfaces of the aluminium blocks. FEA simulations with a variation of the film coefficient showed that a variation of 20% produce temperature variations of > 0.1^oC , which should have been detected.

c) *Heat flow outside the sample volume*

The measured thermal conductivity of the samples varied in the range from 0.16 to 1.2 W/mK. Especially in the region below 0.2W/mK, where the plexiglas-spacer (k=0.19W/mK) had a better conductivity than the material sample, the fraction of the heat flux through the materials surrounding the samples increased rapidly. FEA studies result in 23% for a thermal conductivity of 0.16 W/mK compared to 8% at 0.6 W/mK and 4.2% at 1.25 W/mK. This effect was taken into account by the FEA analysis. Due to the limitation of the finite element granularity, a systematic uncertainty of 4.4 % at 0.16 W/mK, 2.8 % at 0.29 W/mK and 1.0 % for $\geq$ 0.6W/mK are included in the results.

d) *Finite settling down time*

The usual waiting time to achieve thermal equilibrium inside the Styrofoam box was 1.5 to 2 hours due to the large thermal resistance of the foam to the climate chamber. Measurements over a period of up to 15 hours demonstrated that changes of maximal 1 bit = 0.05^oC occurred during this additional time. An uncertainty of maximum 0.6 % is attributed for the different samples.

e) *Thermal profile of the heating and cooling block*

Figure 10 shows the temperature distribution of the heater and the cooling block for water with known thermal conductivity at 1 W. The differences between the hottest and coldest spot on the heating block and cooling block are 0.5^oC and 0.65^oC respectively. Due to the finite conductivity of the aluminium blocks, the heat flux produced a temperature profile on the blocks and the NTC positions have to be taken into account to compare FEA simulations with experimental data. This effect might have influenced the individual temperature measurements by 0.05^oC introducing a systematic uncertainty of 0.1^oC for ΔT. The contribution on ΔR is estimated to be $\leq$ 1.2 %.

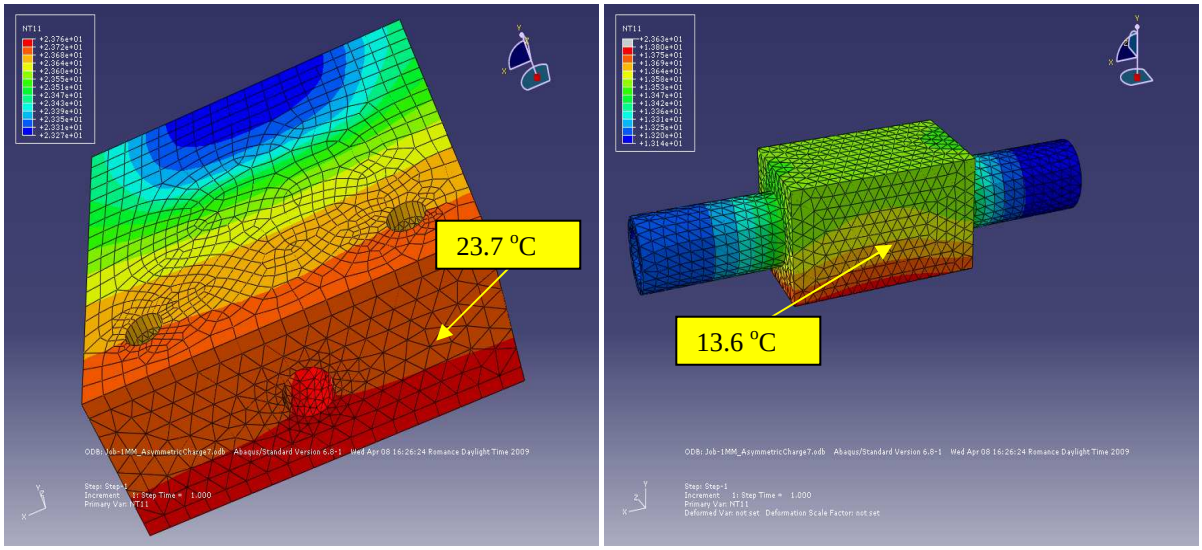

Figure 10: FEA results for water sample. Left: heater block, Right: cooling block. The NTC positions are indicated by the arrows.

f) *Uncertainty of the thermal conductivity for the materials in the set-up*

The values of the thermal conductivity for the materials used in the set-up are known only with a certain precision. For some materials (e.g. Polyimide, Plexiglas, glue-layers, scotch...) this uncertainty is on the level of several percent. In the direct heat path through the samples this could in principle affect the temperature drop through the different layers of the heater film and therefore the comparison with the FEA simulations. This uncertainty contributes with 1.2% to ΔR.

For the samples with very low conductivities the fraction of the heat-flux through the Plexiglas spacer and the double sided scotch would be influenced. A systematic uncertainty of 1.2% will be included in the measurement of silicon oil and 0.5 % in the one of Glycerol. For the other samples this effect was negligible.

g) Temperature dependence of the thermal conductivity

The thermal conductivity is a function of the temperature. The maximum temperature on the heater blocks was 28.5°C (in the case of the silicon oil sample) and the coolant temperature was for all measurements ~ 13°C. The difference ΔT of temperature between the heating and cooling blocks was for all data points in the range 2°C to 14°C. For the samples analyzed in this experiment only H_2O and silicon oil should show a measurable variation of the thermal conductivity in this temperature range.

There was no possibility to measure the thermo-profile through the samples, and for the temperature between the surfaces of the heater and cooling blocks only an average value can be given.

The thermal resistance of the different samples was measured by the variation of the power on the heater blocks. This change of temperature modified the conductivity in the sample. This temperature dependence had been included in the FEA calculations for the H_2O simulation and gives a contribution to the systematic uncertainty of 0.4% for ΔR.

The temperature dependence on the thermal conductivity was not included in the simulation for the silicon oil due to lack of information (see comment in Section 4.4). A systematic uncertainty of 1% for ΔR takes this situation into account.

The systematic uncertainties for the thermal resistance of the different samples are summarized in **Table 3**.

sample	a) geometrical (%)	b) Convection & radiation (%)	c) Heat outside sample (%)	d) Finite time 0.05 °C/ T_{max} (%)	e) Profile blocks 0.1 °C/ T_{max}(%)	f) Materials in set-up (%)	g) Thermo profile sample (%)	Total (%)
Silicon oil L-45 (Union Carbide)	3.2	1	4.4	0.4	0.8	1.7	1 %	5.9
Glycerol	3.2	1	2.8	0.6	1.2	1.3	none	4.8
H2O.	3.2	1	1	0.5	1	1.2	0.4 %.	3.9
DC340 (Dow Corning)[8)]	3.2	1	1	0.6	1.2	1.2	none	3.9
DC 340 irradiated[9)]	5.6	1	none	0.6	1.2	1.2	none	6.0
WLPG irradiated	3.2	1	1	0.6	1.2	1.2	none	3.9
WLPG (Fischer)	3.2	1	1	0.6	1.2	1.2	none	3.9
CGL 7018 (AI Technology)[10)]	3.2	1	1	0.6	1.2	1.2	none	3.9

Table 3: Contributions to the systematic uncertainty of R for the different materials measured.

4.7 Overall consistency check

The correlation between the thermal conductivity k and the thermal resistance $\Delta T/P$ of the different samples was fitted by the potential function $k = 10.262 * (\Delta T/P)^{-1.2272}$ (see Figure 11). The difference from the purely geometrical correlation $k = (\text{thickness/area}) * (\Delta T/P)^{-1}$ reflects the variation of the heat flux through the samples relative to the flow through the surrounding materials (Plexiglas-spacer and double-sided scotch). The residuals between the geometrical correlation and the fit are 28.5 % at 0.16 W/mK, 8.7% at 0.6 W/mK and 4.6% at 1.25 W/mK. These values can be compared with the FEA calculations of the effective heat flux through the samples and provide a consistency check for the performance of the set-up and the estimation of the systematic uncertainties over the whole rage of the measured thermal conductivities. This fit showed a difference of 5.5 % at 0.16 W/mK, 0.7% at 0.6 W/mK and 0.4% at 1.25 W/mK compared to the heat flux through the Plexiglas spacer and the double sided scotch (Section 4.6c).

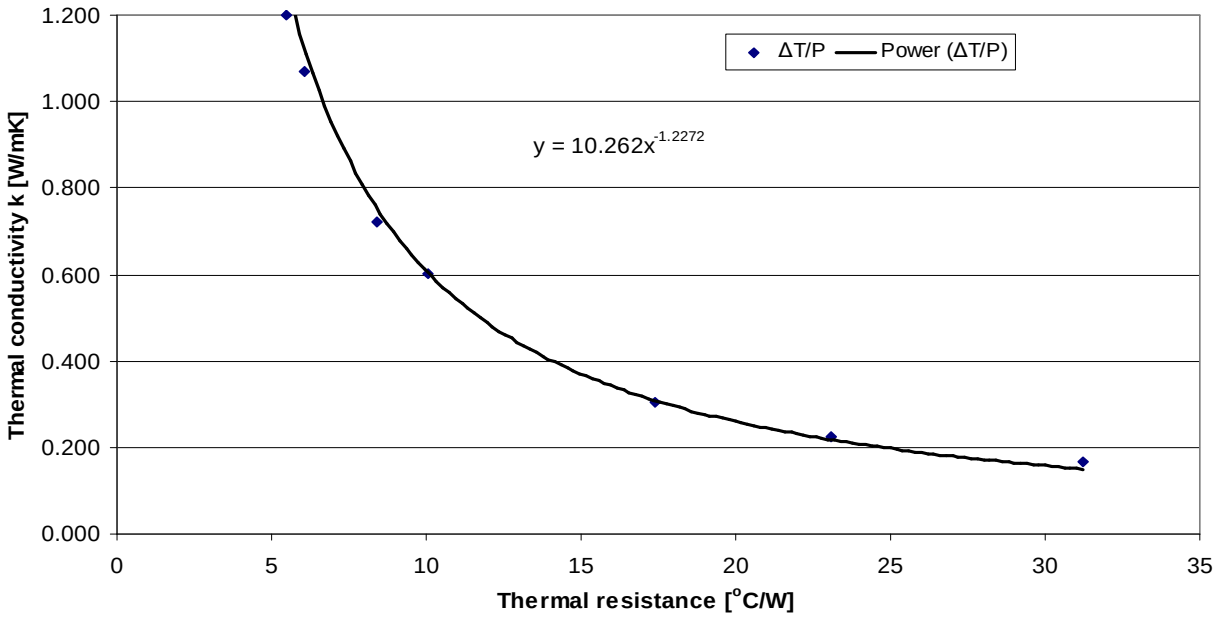

Figure 11: Correlation between the thermal resistance and the thermal conductivity in the set-up.

This function allows a simple projection of the thermal resistance error ΔR on the thermal conductivity axis over our entire resistance range: $\Delta k/k = 1.2272 \times \Delta R/R$.

5. IRRADIATION OF GREASE SAMPLES & RESULTS

Two compounds were selected for the irradiations:

- DC340[5)] (Dow Corning): A grease that was used for the existing SCT and was considered to be the best candidate when earlier selected and tested at that time.

- WLPG[9)] (Fischer): A non-silicon grease with an attractive thermal performance (quoted by the manufacturer data sheet as ~10 W/mK).

The two different samples were irradiated inside a container with the same volume. The size of the container was 10 mm diameter and 50 mm in length which correspond to a volume of ~3.9 cm^3. The total weight was ~8.2 g in case of the DC340 and ~5 g for the graphite loaded WLPG compound.

The irradiations took place in 2008 at CERN PS T7 with a 24 GeV/c primary proton beam. A special Plexiglas container had been prepared (see Figure 12). The beam cross section was about 15 x 15 mm^2 (FWHM). The container of 10 mm diameter was aligned with the beam axis to obtain a uniform irradiation within ~90% along the full length.

Figure 12: Plexiglas containers for the grease irradiation at 10^{15} 1 MeV n_{eq}/cm^2.

In order to obtain a flux of 10^{15} n_{eq}/cm^2 at 1 MeV, the samples were irradiated with the proton beam to $1.5x10^{15}$ p/cm^2 at an average rate of 10^{13} p/hour. The total irradiation period was ~ 6 days.

After irradiation the grease samples were stored inside the PS irradiation facility until the radioactivity decreased to a reasonable level.

Apart from the thermal conductivity measurements reported in Section 4.4, two interesting observations were made: the consistency of the sample and the radioactivity level after such fluence.

Concerning the first observation, the DC340 which was originally pasty polymerized into a single and elastic block similar to a silicon rubber (see Figure 13). A change of the consistency had also been reported earlier[11)] after an exposure to $1x10^{15}$ p/cm^2. The Fischer WLPG carbon loaded grease could be partly extracted and its consistency was dry and pasty as part of the oil was lost during the irradiation and storage time (see Figure 6). Depending of its use, the mechanical properties of the DC340 may be unsatisfactory. The mechanical characteristics of WLPG are not satisfactory, due to the loss of oil already noticed when received from the provider in its original container. The oil separation certainly depends on the storage and usage temperature.

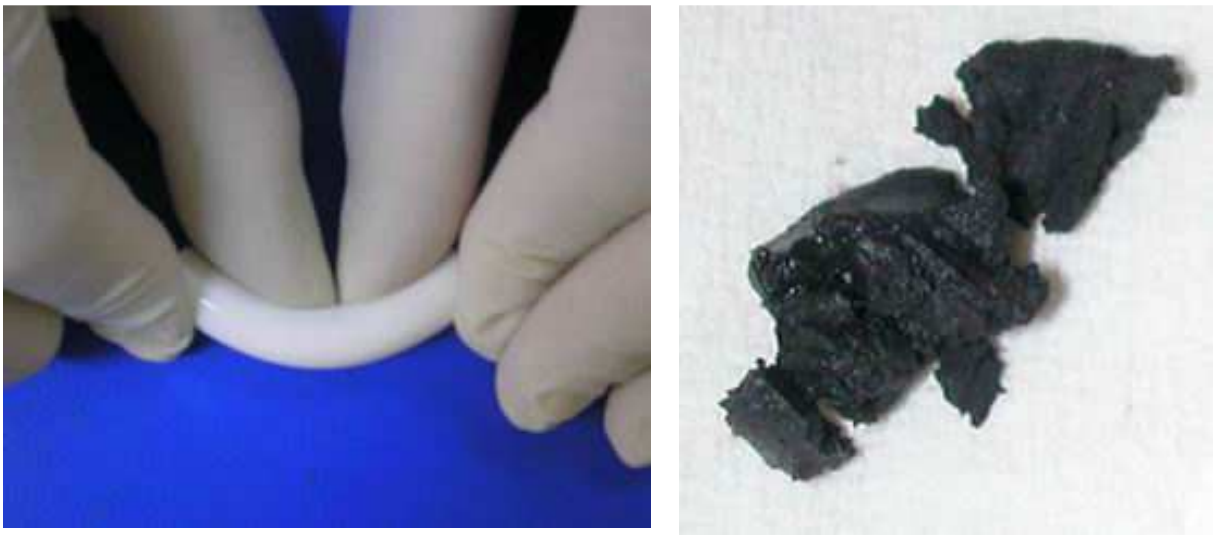

Figure 13: Samples out of the Plexiglas container after irradiation at a fluence of $1.5x10^{15}$ 24 GeV protons. Left: DC340. Right: WLPG.

The second observation concerns the measured radioactivity level (see Table 4). The activity of carbon loaded grease (WLPG) was at least 10 times lower than that of the DC340 compound. It could already be measured 2 days after the end of the irradiations while it took ~2 months for the DC340.

	DC340	**WLPG**
Activity measured after [days]	65	2
Activity at 10cm (with Plexiglas) [μSv/h]	5	0.5
Activity against Plexiglas (at 0cm) [μSv/h]	100	7

Table 4: Induced radioactivity measurements of the 2 samples: The activity was measured at different times after the irradiation, for the 2 samples.

6. CONCLUSIONS

Direct measurements of the thermal conductivity have been made for several materials that are being considered as a thermal interface between the modules and cooling pipes, in one of the Inner Tracking Detector (ID) designs for the upgraded ATLAS detector.

The measurements have been made, in the range 0.16 to 1.2 W/mK and with a precision of 4.8-7.4%, using a custom built apparatus that compares the conductivity of materials in two parallel channels. The measured thermal conductivity of water and glycerol are in good agreement with the well established quoted values[15)] for these materials. This gives a good confidence that the systematic uncertainties are limited to the estimated level.

The limitations of the actual set-up have been demonstrated in the compilation of the systematic uncertainties. The common biggest uncertainty is due to the use of scotch films and the resulting geometrical uncertainties. Solid glue layers of defined thickness should solve this problem in future measurements.

The thermal behaviour of the two tested samples remains within specifications after irradiation (the CGL7018 sample has not yet been irradiated).

The mechanical properties of the DC340 and Fischer WLPG compounds are less satisfactory. The polymerisation of the DC340 compound shows that the mechanical tension-free sliding of the modules during heating-up or cooling-down may not be guaranteed following the expected fluence at LHC. This needs further study. The Fischer WLPG sample also showed a modification of the consistency. The important loss of oil during a period of ~1 week and the soiling of the target-station demonstrated the risk of long-term corrosion of the associated electronics due to oxidizing vegetable oil. Other compounds need to be investigated.

Clear evidence is obtained that the specifications of the producers of the three thermal compounds measured are not reliable and must be verified before use. As an example, different DC340 production sites announce different numerical values for a product which is commercialized under the same name (“made in China” is quoted k = 0.42W/mK, “made in US” is quoted k = 0.59 W/mK).

Our measurement of CGL7018 gave a higher value than earlier measurements of the ATLAS group[11)12) 12)] and the result from the ALICE collaboration[13)]. However it is less than a recent measurement of k = (1.47 $\pm$ 0.08) W/mK, using the Line Source Thermal Conductivity Probe (LSTCP) method[14)].

These measurements also provided the possibility to test the accuracy of the FEA-simulations, which were used to calculate the thermo-mechanical behaviour of the silicon-detector modules. The excellent agreement of our results for H_2O and Glycerol demonstrate that the thermal behaviour is correctly described by our FEA simulations.

The thermal grease study dedicated for the upgrade module program is essential for the selection of a thermal compound that will provide a satisfactory sliding join before and after irradiations of an equivalent fluence of 1.10^{14} 1Mev n_{eq}/cm^2. So far the silicon based gel and the organic oil based compounds are not satisfactory. Several other non-silicon based compounds are being considered. The mechanical and thermal ageing properties as well as the radiation hardness will have to be proven satisfactory for the ATLAS strip tracker upgrade operation.

Acknowledgments:

We acknowledge the support of Maurice Glaser, from CERN PH/DT, for his help with the irradiation work at PS T7. He kindly helped with the irradiation of the two grease samples and provided the storage and the measurements of the activity level after irradiation.

References:

1. A. Abdesselam *et al., Nucl. Instr. and Meth. Phys. Res. A* **568** (2006), p. 642
2. A. Abdesselam et al, *Nucl. Instrum. Methods Phys. Res., A* **575** (2007), p. 353-389
3. K. Nagano, *ATL-UPGRADE-PROC-2009-002*
4. Y. Unno, A. Clark, K. Jakobs, G. Taylor, C. Garcia, K. Hara, R&D towards the Module and Service Structure design for the ATLAS Inner Tracker at the Super LHC (SLHC), *ATU-RD-MN-0007*
5. Dow Corning DC340 heat sink compound, *http://www.dowcorning.com*
6. Polyimide Thermofoil Heaters, Minco, http://*www.minco.com*
7. ABAQUS, A FEA simulation tool from Simulia Dassault Systèmes, *http://www.simulia.com/*
8. CATIA, A CAD software for mechanical engineering design from Dassault Systèmes, *http://www.3ds.com/products/catia/welcome/*
9. Fischer WPLG thermal heat sink compound, *http://www.fischerelektronik.de*
10. AI Technology, CGL7018 heat sink compound, http://*www.aitechnology.com*
11. ATLAS Pixel Detector, *Technical Design Report* (k = 1.5 W/mK), p203
12. C. Gemme, W. Dietsche, E. Vigeolas, *Pixel week* June 2002, *http://www.ge.infn.it/ATLAS/Test/Adhesives/ptotocols/Glue_Selection.pdf* (k = 0.6 W/mK)
13. IMTC 2004 - *Instrumentation and Measurement Technology Conference Como*, Italy 18-24 May 2004 (AIT CGL7018 k = (0.7 $\pm$ 0.1) W/mK) (nominal k = 4 W/mK)
14. T. Jones, Measurement of the thermal conductivity of CGL7018 by the LSTCD Method k = (1.47 $\pm$ 0.08) W/mK *https://twiki.cern.ch/twiki/pub/Sandbox/TrackerExchange/LSTCP_CGL7018.pdf*
15. Handbook of Chemistry and Physics, *CRC press*